NASA TM X-56028

AERODYNAMIC DRAG REDUCTION TESTS ON A FULL-SCALE TRACTOR-TRAILER
COMBINATION WITH SEVERAL ADD-ON DEVICES

Lawrence C. Montoya and Louis L. Steers
NASA Flight Research Center

December 1974

A cooperative study between

NASA Flight Research Center   DOT Transportation Systems Center
Edwards, California 93523   Cambridge, Massachusetts 02142

1. Report No. TM X-56028	2. Government Accession No.	3. Recipient's Catalog No.
4. Title and Subtitle AERODYNAMIC DRAG REDUCTION TESTS ON A FULL-SCALE TRACTOR-TRAILER COMBINATION WITH SEVERAL ADD-ON DEVICES		5. Report Date December 1974
		6. Performing Organization Code
7. Author(s) Lawrence C. Montoya and Louis L. Steers		8. Performing Organization Report No.
		10. Work Unit No. 770-18-10
9. Performing Organization Name and Address NASA Flight Research Center P. O. Box 273 Edwards, California 93523		11. Contract or Grant No.
		13. Type of Report and Period Covered Technical Memorandum
12. Sponsoring Agency Name and Address National Aeronautics and Space Administration Washington, D. C. 20546	U.S. Department of Transportation Office of the Secretary Office of the Assistant Secretary for System Development and Technology Washington, D. C. 20590	
		14. Sponsoring Agency Code

15. Supplementary Notes

The results presented herein were presented at the Reduction of Aerodynamic Drag of Trucks Conference, California Institute of Technology, Pasadena, California, October 10 to 11, 1974.

16. Abstract

Aerodynamic drag tests were performed on a conventional cab-over-engine tractor with a 45-foot trailer and five commercially available or potentially available add-on devices using the coast-down method. The tests ranged in velocity from approximately 30 miles per hour to 65 miles per hour and included some flow visualization. A smooth, level runway at Edwards Air Force Base was used for the tests, and deceleration measurements were taken with both accelerometers and stopwatches. This paper presents an evaluation of the drag reduction results obtained with each of the five add-on devices.

17. Key Words (Suggested by Author(s)) Aerodynamic drag Tractor-trailer Add-on devices	18. Distribution Statement Unclassified – Unlimited	
19. Security Classif. (of this report) Unclassified	20. Security Classif. (of this page) Unclassified	21. No. of Pages 24	22. Price

AERODYNAMIC DRAG REDUCTION TESTS ON A FULL-SCALE

TRACTOR-TRAILER COMBINATION WITH

SEVERAL ADD-ON DEVICES

Lawrence C. Montoya and Louis L. Steers
Flight Research Center

INTRODUCTION

Because of the recent fuel oil crisis, the conservation of fuel oil products has become a matter of greater concern to everybody. The resulting high prices and sometimes limited quantities of gasoline and diesel fuel have caused increased interest in ground vehicle efficiency. In the past, when ground vehicle fuel was comparatively inexpensive and readily available, the aerodynamic drag (wind resistance) of some high volume carriers during design was considered unimportant. The high aerodynamic drag of these designs (i.e., box shapes) was merely overcome by more powerful engines, with resulting increases in fuel consumption.

In the fall of 1973, in response to the fuel crisis and increased interest in the aerodynamic drag of ground vehicles, the NASA Flight Research Center began a drag reduction program on a representative box-shaped ground vehicle (refs. 1 and 2). After baseline data were obtained for the vehicle with all square corners, the vehicle was modified by rounding the corners and sealing the undercarriage. The resulting reduction in aerodynamic drag exceeded 50 percent, which is equivalent to a fuel savings of approximately 15 percent to 25 percent at highway speeds.

Another aerodynamic drag ground vehicle study was initiated in the spring of 1974. Sponsored jointly by NASA and the Department of Transportation, the program was to assess the performance gains on a tractor-trailer combination due to the addition of different low cost drag reduction devices. These add-on devices, which are commercially available, or potentially available, were developed by private business concerns to reduce the aerodynamic drag of existing tractor-trailer combinations with only minor modifications.

A representative cab-over-engine tractor-trailer combination without any devices attached (the basic vehicle) was tested first. The tests were then repeated with the add-on devices installed.

This paper presents an evaluation of the drag reduction results obtained with each of five add-on devices using the coast-down technique.

SYMBOLS

A	frontal cross-sectional area (does not include the undercarriage and tires), 94 square feet
C_{D_a}	aerodynamic drag coefficient, $\dfrac{D_a}{qA}$
D	drag
g	local acceleration of gravity
q	dynamic pressure, $0.5\rho V^2$
Δt	time increment
V	velocity
ΔV	velocity increment
W	vehicle weight during each test
x	distance between back of cab and front of trailer, 40 inches or 62 inches
ρ	air density

Subscripts:

a	aerodynamic
m	mechanical
t	total

TEST VEHICLE

The tractor-trailer combination test vehicle (fig. 1) consisted of a cab-over-engine tractor and a 45-foot-long, two-axle, smooth-sidewall trailer. The front vertical corners of the trailer had a 12-inch radius. The total gross weight of the test vehicle was approximately 32,000 pounds. General specifications of the test vehicle are given in table 1.

2

METHOD

The drag data were obtained by using the coast-down method under carefully controlled conditions. Tire pressure was kept nearly constant by filling the tires with nitrogen, which reduces temperature effects. Vehicle weight was determined for each day of testing and was not permitted to vary significantly to keep mechanical or rolling drag as constant as possible between tests. By keeping mechanical drag constant, any changes in drag resulting from the addition of the devices would be aerodynamic in origin.

For this study, total drag is considered to be the retarding force that can be directly derived from the deceleration of the vehicle. The components of the total drag and its definition are as follows:

$$D_t = D_m + D_a = \frac{\Delta V}{\Delta t} \frac{W}{g}$$

where the total drag is the sum of the mechanical drag (D_m) and aerodynamic drag (D_a). By setting the manual transmission in neutral during each deceleration run, the mechanical drag consisted of (1) the tractive drag of the tires and bearings and the gear resistance back through the drive line to the transmission and (2) the thrust from the rotational inertia of the wheels and tires.

The test vehicle was accelerated to a few miles per hour above the starting velocity of each test, and the manual transmission was then disengaged. The time it took for the truck to slow to given speeds was recorded and used to calculate the total drag from the above-stated definition. A more complex approach to the coast-down method is described in reference 3.

TEST CONDITIONS

The tests were conducted on an Edwards Air Force Base runway, which had a concrete surface with a constant elevation gradient of 0.125 percent. The effect of this small gradient was eliminated by averaging successive runs in opposite directions. The tests ranged in velocity from approximately 30 miles per hour to 65 miles per hour. Most of the tests were made in calm wind conditions.

During the tests, ambient pressure, temperature, and wind velocity and direction were recorded.

Tests were performed with a gap of either 62 inches or 40 inches between the front of the trailer and the back of the top part of the cab (fig. 1).

During the first tests, it was found that the position of the thermostatically controlled radiator cooling shutters had a considerable effect on the drag measurements.

To eliminate this variable, a cover that prevented airflow through the shutters was put over the radiator opening before each run (fig. 2).

INSTRUMENTATION

A ±0.1g accelerometer with 0.001g resolution was used to measure deceleration along with a bank of five 0.1-second stopwatches and a calibrated precision speedometer with a 0.1-mile-per-hour readout capability. The speedometer was driven by a fifth wheel. The velocity and distance of the fifth wheel was displayed digitally inside the truck's cab (fig. 3) along with the bank of stopwatches. The time increments corresponding to preselected velocity intervals in miles per hour (i.e., 60 to 55, 55 to 50, 50 to 45, 45 to 40, and 40 to 35) were obtained by starting all the stopwatches simultaneously at the starting test velocity and stopping them individually at the end of the desired velocity interval. The stopwatch data were hand recorded. The accelerometer and fifth wheel velocity outputs were recorded on tape and identified with an event marker during each test.

DEVICES TESTED

The five add-on devices which were tested are shown as the crosshatched areas in figure 4.

Three of the devices (devices A, B, and E) were cab mounted and designed to deflect more of the flow over the trailer. The other two devices (devices C and D) were mounted on the trailer. It appears that device C was designed to make the air flow smoothly around the trailer, and apparently device D was designed to maintain attached flow over the top of the trailer.

Device A, which was cab mounted, was 67 inches wide and 32 inches high. Device B, also cab mounted, was 52 inches wide and 27 inches high, with a 6.5-inch gap between the device and the cab. Device C was trailer mounted and extended a maximum of 24 inches forward of the trailer. Device D was mounted on the top front edge of the trailer, with a 6-inch gap between the front edge of the device and trailer and a 1.5-inch gap between the rear edge of the device and trailer. Device E was 60 inches wide, cab mounted, and extended vertically 48 inches above the cab in the stored position and 38 inches above the cab in the fully deployed position, which is shown in figure 4. The deployment and storage of device E were automatic and depended on the impact pressure and its variation with velocity. Data for this device were acquired only for the fully deployed position and the rear trailer location (62-in. gap).

The manufacturers chose the device of the best size available at the time of purchase for the test vehicle. All the devices were installed according to manufacturer's instructions.

RESULTS

Baseline Configuration

Typical results for the baseline configuration from several stopwatch runs and one accelerometer run are shown in figure 5 in terms of total drag versus truck velocity. The data show that the two methods of measuring deceleration (i.e., stopwatch precision speedometer and accelerometer) are consistent with each other. Repeatability is shown by the stopwatch data, which were obtained on separate days by two different people.

Baseline data for the two trailer positions (gaps of 62 in. and 40 in.) are presented in figure 6. It is apparent that the total drag was lower when the distance between the cab and trailer was shorter. At 55 miles per hour, the total drag was reduced approximately 7 percent, which is equivalent to a reduction in aerodynamic drag of approximately 10 percent.

Modified Configurations

The total drag with the various add-on devices installed is shown in figures 7(a) to 7(e). In figures 7(a) to 7(d) the crosshatched region represents the drag range for the baseline vehicle; the lower bound is for the 40-inch gap and the upper bound is for the 62-inch gap. In figure 7(e) baseline data for only the 62-inch gap are shown because device E was tested only with a 62-inch gap.

The difference in total drag between the modified and baseline configurations is summarized in figure 8 for the two trailer positions at a speed of 55 miles per hour. As shown, the total drag reduction ranged from 18 percent for device A for the rear trailer position to approximately 2 percent for device D for both trailer positions. (The letters A, B, and so forth were assigned to the devices according to the chronological testing sequence and not according to rank.)

As mentioned before, total drag consisted of aerodynamic plus mechanical drag. The tractive portion of the mechanical drag is shown in figure 9. The data point at approximately 1 mile per hour represents a value that was measured using two methods, the coast-down and tow methods, and the solid curve extrapolation is based on Hoerner's semiempirical equation for rolling resistance (ref. 4). Using these data and accounting for the thrust from the rotational inertia of the wheels and tires, the aerodynamic drag was calculated by the relationship given on page 3. The resulting values of aerodynamic drag reduction are listed in table 2 together with the corresponding drag coefficients, C_{D_a}, for the two trailer positions. The drag coefficients were based on a frontal cross-sectional area of 94 square feet, which does not include the projected areas of the undercarriage and tires. The aerodynamic drag reduction ranged from 24 percent for device A for the rear trailer position to 2 percent for device D for the forward trailer position.

As shown in table 2, the drag coefficients range from 1.17 for the baseline configuration for the rear trailer position to 0.89 for device A for both trailer positions. The drag coefficients obtained from wind tunnel tests (refs. 5 and 6) for cab-over-engine tractor-trailer combinations in the baseline configuration range from approximately 0.9 at the high end (i.e., approximately the same as the full-scale vehicle of this study with the best add-on device) to approximately 0.7 at the lower end. The drag coefficients from reference 5 are based on a frontal projected area and in reference 6 on the area based on the trailer's height above the ground times the width. A direct comparison with the results of either of these studies is not possible because of model configuration differences that are not readily definable (e.g., cab height, trailer size, corner radius, and distance between trailer and tractor).

A full-scale drag coefficient of approximately 1.04 is obtained for the baseline configuration of this study if the tire rolling resistance data of reference 7 (rotating drum tests) are applied instead of the extrapolation for velocity effects from reference 4. This drag coefficient is still above 1, whereas the majority of the wind tunnel data are well below 1.

Effect of Crosswinds

The data presented thus far are for zero wind conditions. Limited data were also obtained with crosswinds for the basic configuration and for some modified configurations. These data show that the drag of the configurations with add-on devices was sensitive to crosswinds, whereas the drag of the basic configuration exhibited little if any change. Figure 10 presents the total drag results for a 2- to 3-mile-per-hour crosswind at an angle of 11° relative to the longitudinal axis of the vehicle for the basic configuration and devices A, B, and C. These results are for the rear trailer position and represent the average of runs in two directions. Although the data do not define wind effects in detail, they indicate that in general the crosswinds reduced the ability of the add-on devices to decrease drag.

Figure 11 compares the total drag reduction due to the add-on devices for the rear trailer position as determined under conditions of crosswinds and zero wind (fig. 8). The total drag reduction decreased from 18 percent to 16 percent for device A, from 11 percent to 4 percent for device B, and from 8 percent to 6 percent for device C. These data were limited and should be substantiated by additional testing.

Flow Visualization

Some flow visualization pictures were taken of the truck at approximately 55 miles per hour (figs. 12(a) to 12(f)). The airflow was made visible with powder (diatomaceous earth), which was emitted at the top front edge of the cab. The powder was pumped out of a sandblaster hopper inside the trailer. Although the photographs do not define the details of the stream tube paths, they give a general idea of the flow's behavior with and without the add-on devices. It should be noted that the diatomaceous earth used in figures 12(a) and 12(e) produced a low density dispersion. The same general flow pattern resulted when diatomaceous earth that

produced a high density dispersion was used. Crosswinds ranged from 2 miles per hour to 5 miles per hour when the pictures were taken.

CONCLUDING REMARKS

This study showed that moving the trailer forward from 62 inches to 40 inches reduced the aerodynamic drag for the baseline configuration approximately 10 percent at zero wind conditions.

The maximum aerodynamic drag reduction realized from an add-on device at zero wind conditions was approximately 24 percent for the rear trailer position (62 in.). Some add-on devices provided only small reductions in drag.

Limited data obtained for some of the devices showed that their ability to decrease drag was reduced by the presence of crosswinds.

Flight Research Center
National Aeronautics and Space Administration
Edwards, Calif., December 9, 1974

REFERENCES

1. Saltzman, Edwin J.; and Meyer, Robert R., Jr.: Drag Reduction Obtained by Rounding Vertical Corners on a Box-Shaped Ground Vehicle. NASA TM X-56023, 1974.

2. Saltzman, Edwin J.; Meyer, Robert R., Jr.; and Lux, David P.: Drag Reductions Obtained by Modifying a Box-Shaped Ground Vehicle. NASA TM X-56027, 1974.

3. White, R. A.; and Korst, H. H.: The Determination of Vehicle Drag Contributions from Coast-Down Tests. SAE 720099, Jan. 1972.

4. Hoerner, Sighard F.: Fluid-Dynamic Drag. Publ. by the author (148 Busteed Dr., Midland Park, N. J.), 1965.

5. Flynn, Harold; Kyropoulos, Peter: Truck Aerodynamics. SAE Transactions 1962, Vol. 70, c.1962, pp. 297-308.

6. Sherwood, A. Wiley: Wind Tunnel Test of Trailmobile Trailers. Wind Tunnel Rept. No. 85, Univ. Maryland, June 1953.

7. Davisson, J. A.: Design and Application of Commercial Type Tires. SP-344, SAE, Jan. 1969.

TABLE 1.—VEHICLE CHARACTERISTICS

The tractor-trailer combination used in this study was one of many that could have been used. Specifications are given herein for completeness only.

Tractor:
  Make . . . . White Freightliner
  Year 1974
  Type . . . . Cab over engine (with sleeper)
  Number of axles 3
  Tire size 10.00-22
  Engine—
    Type . . . . 350 Cummings Turbocharged
    Model NTC-350
    Displacement, in^3 855
    Horsepower at 2100 rpm 310
  Transmission—
    Type . . . . Fuller Roadranger
    Model RTO-9513
Trailer:
  Make . . . . Strick
  Year 1972
  Length, ft 45
  Type . . . . Smooth sidewall
  Number of axles 2
  Tire size 10.00-22

TABLE 2.—AERODYNAMIC DRAG REDUCTION AND DRAG COEFFICIENTS

55 mph, zero wind conditions

Configuration	x, in.	Aerodynamic drag reduction, percent	Drag coefficient
Baseline	62	--	1.17
	40	--	1.06
Device A	62	24	0.89
	40	16	0.89
Device B	62	14	1.00
	40	11	0.94
Device C	62	11	1.04
	40	11	0.94
Device D	62	3	1.13
	40	2	1.04
Device E	62	19	0.95
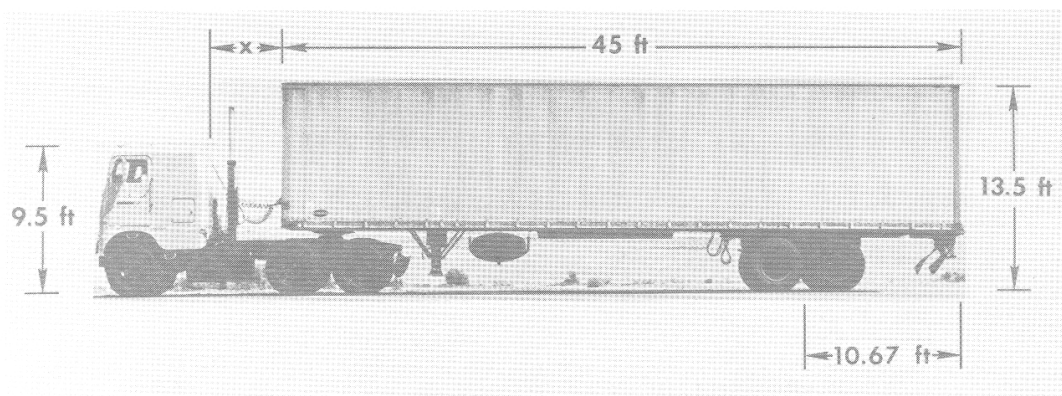
(a) Side view.   E-27320
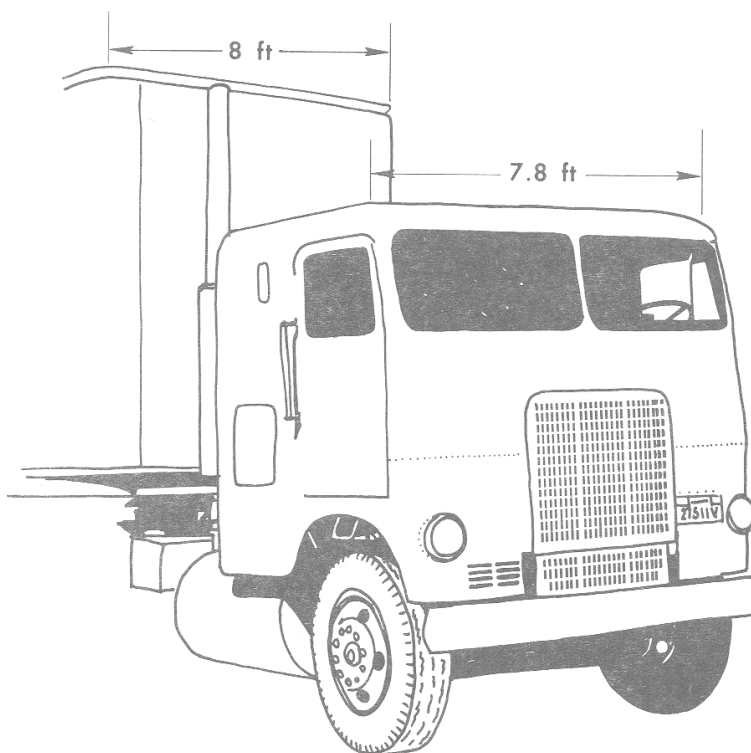
(b) Three-quarter front view.

Figure 1. Test vehicle.

COVER

Figure 2. Cover over radiator opening.   E-27619
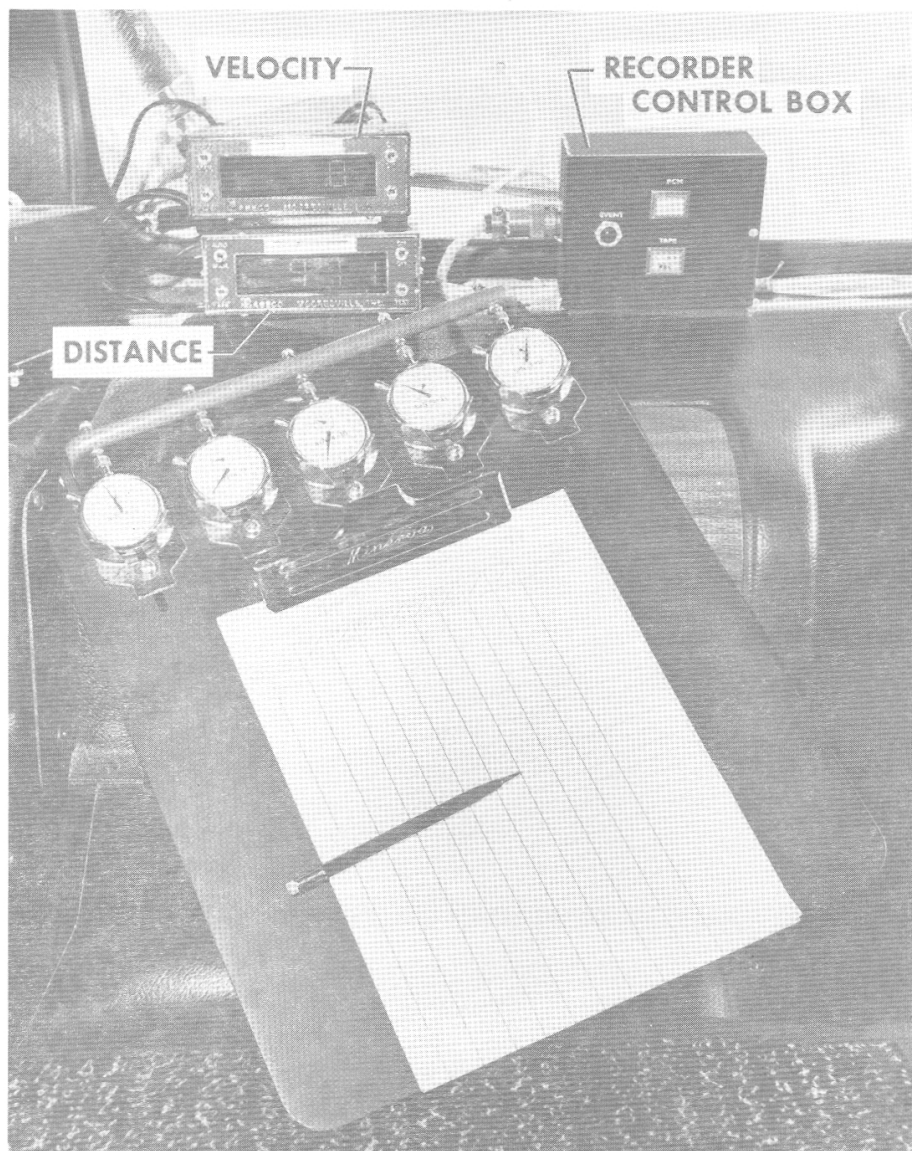
Figure 3. Instrumentation layout inside cab.   E-27851
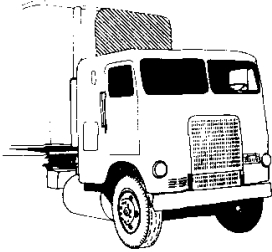
DEVICE A
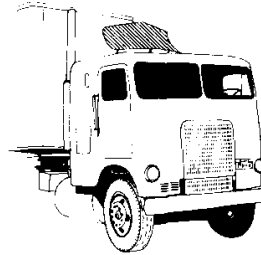
DEVICE B
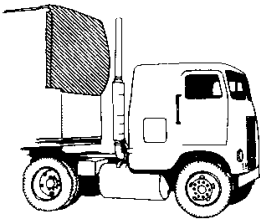
DEVICE C
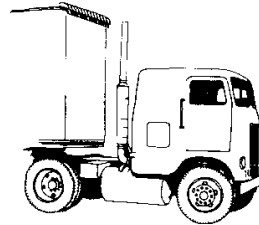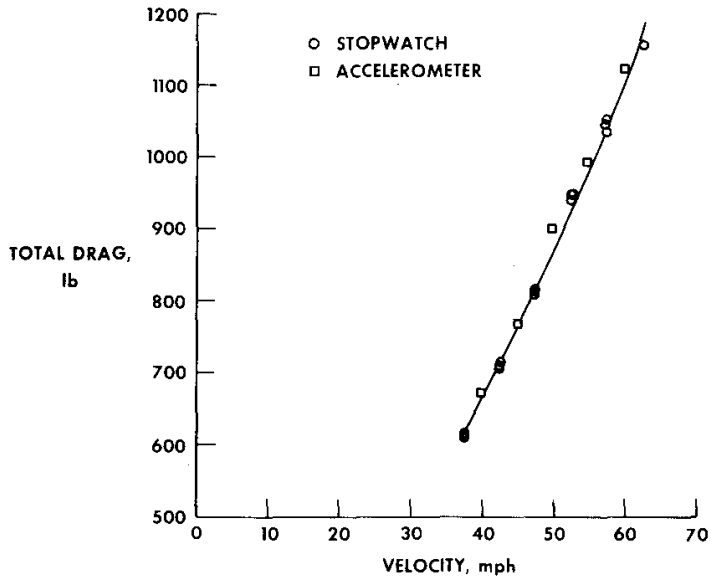
DEVICE D
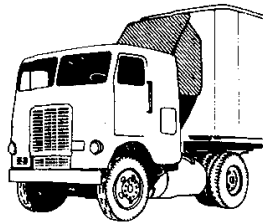
DEVICE E

Figure 4. Devices tested.

Figure 5. Typical total drag for baseline configuration. x = 62 inches, zero wind conditions.
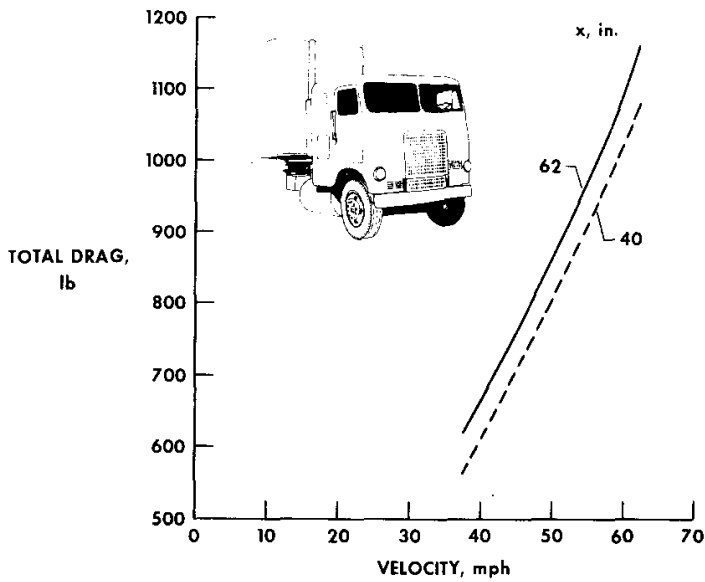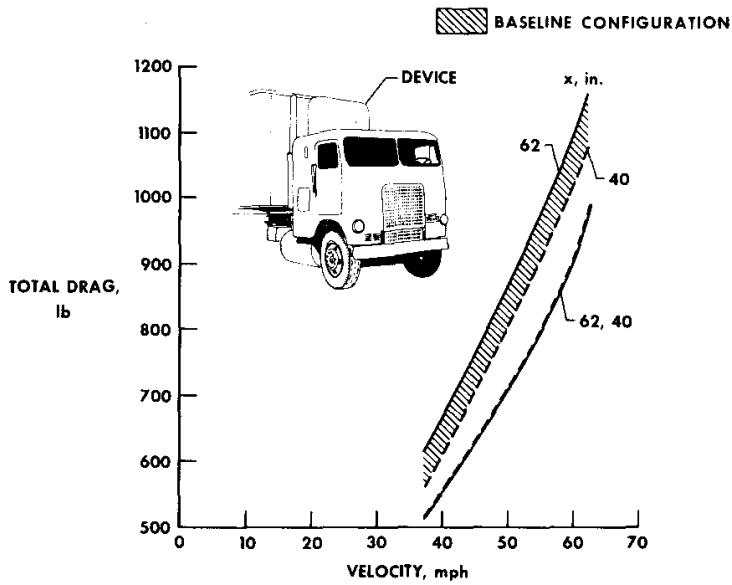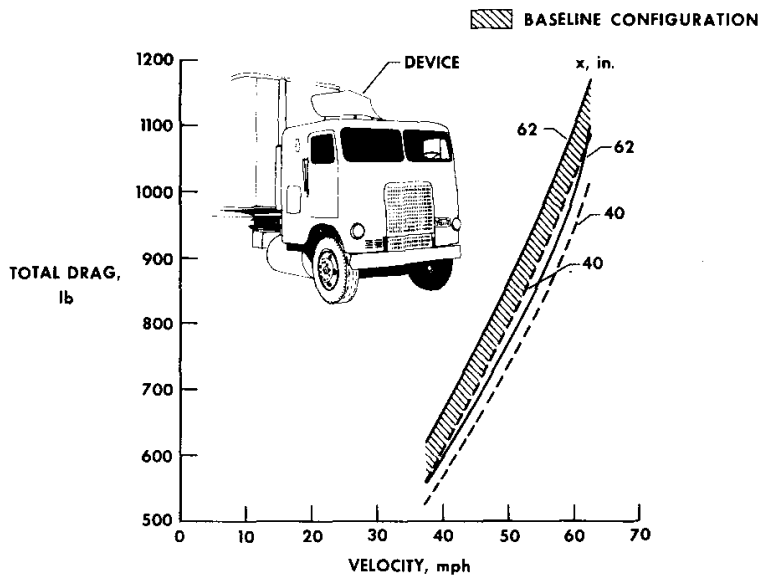

Figure 6. Total drag for baseline configuration for two trailer positions. Zero wind conditions.

TOTAL DRAG, lb

DEVICE

x, in.

62

40

62, 40

VELOCITY, mph

(a) Device A.

TOTAL DRAG, lb

DEVICE

x, in.

62

62

40

40

VELOCITY, mph

(b) Device B.

Figure 7. Comparison of total drag with and without add-on devices.
Zero wind conditions.
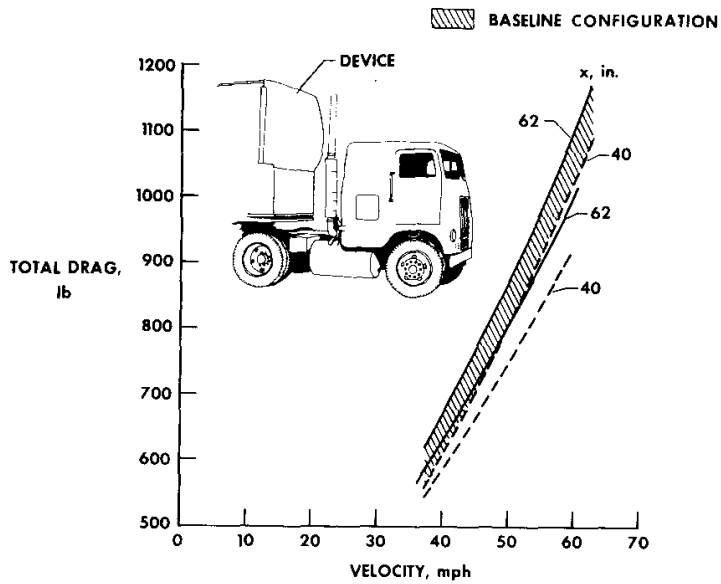
(c) Device C.
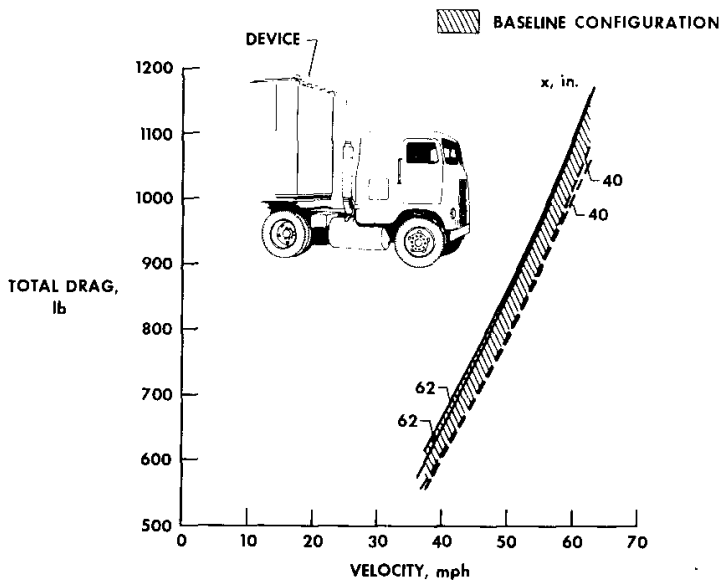
(d) Device D.

Figure 7. Continued.

16
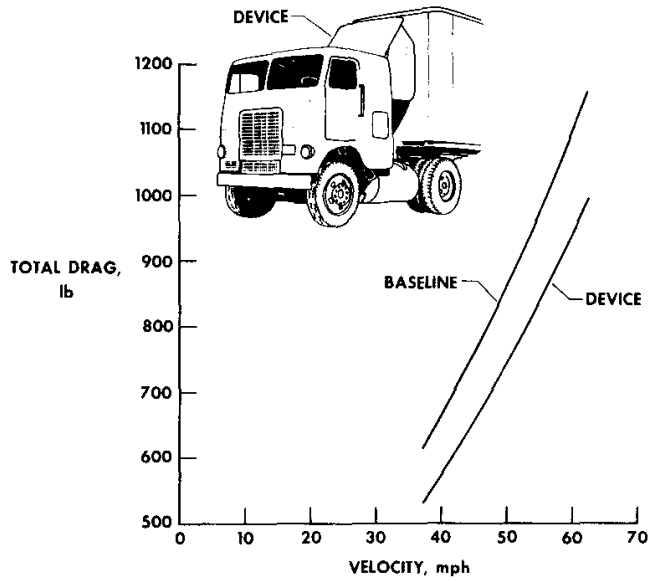
(e) Device E. $x = 62$ inches.

Figure 7. Concluded.
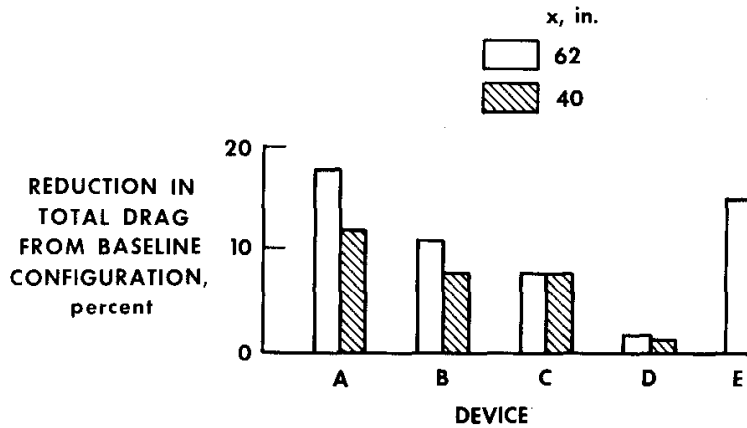
Figure 8. Reduction in total drag for the devices. $V = 55$ miles per hour, zero wind conditions.
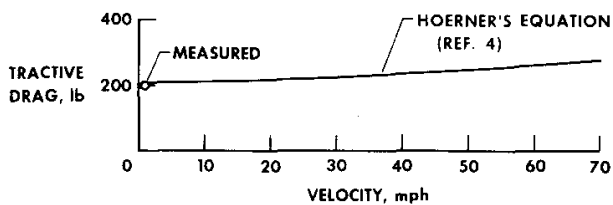
Figure 9. Tractive drag.
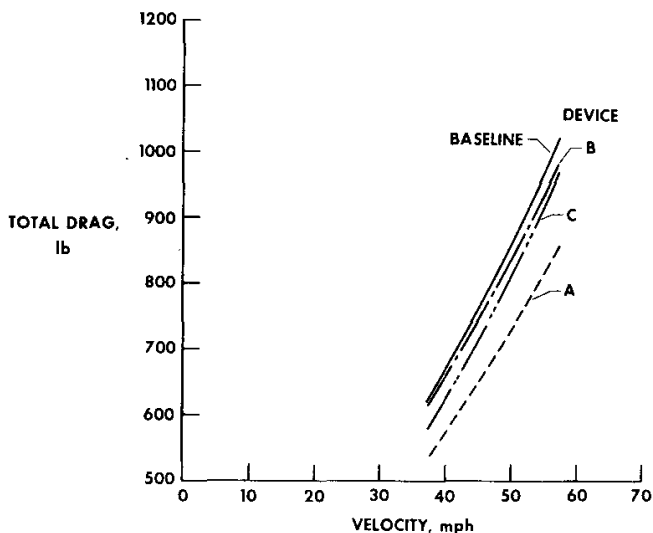
Figure 10. Total drag with crosswinds of 2 miles per hour to 3 miles per hour at an angle of 11°. $x = 62$ inches.
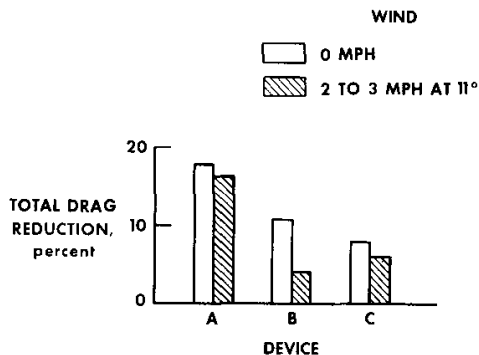
Figure 11. Reduction in total drag for devices A, B, and C with and without crosswinds. $x = 62$ inches; $V = 55$ miles per hour.
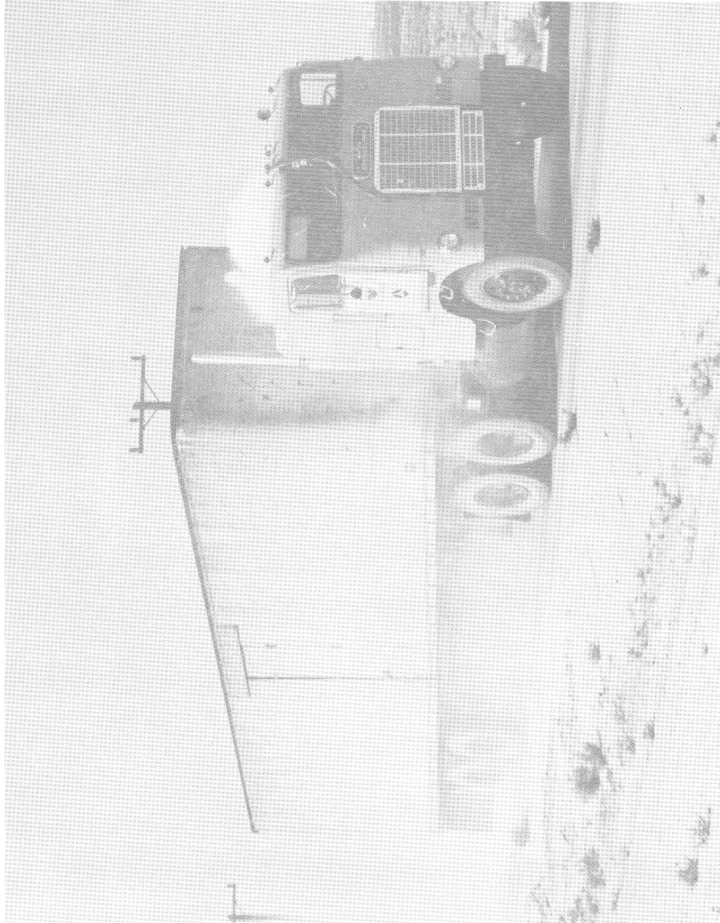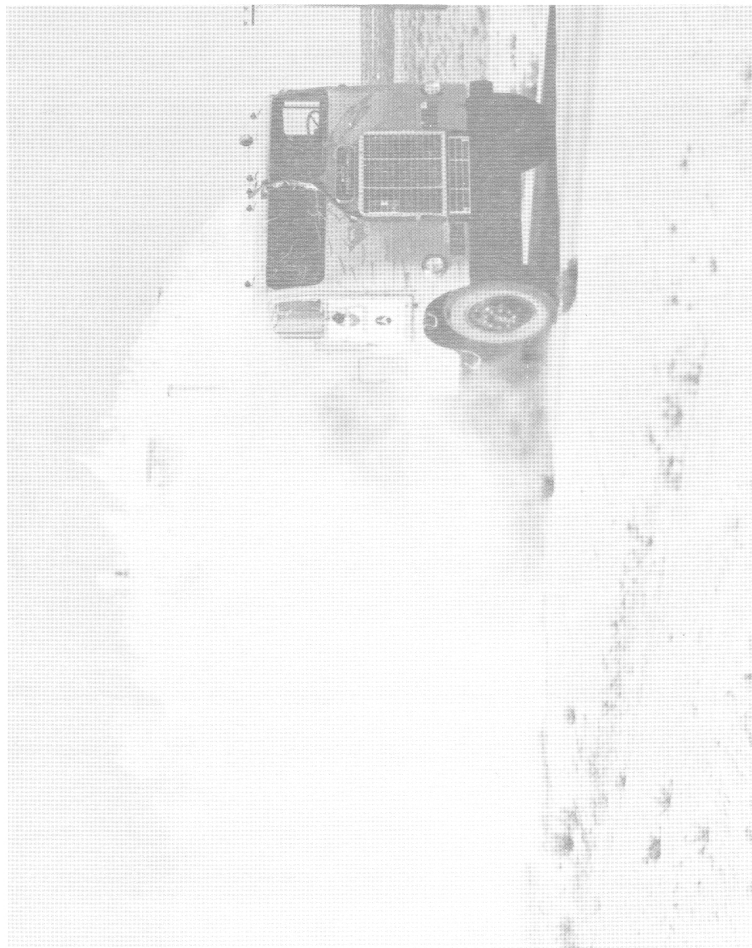
(a) Baseline configuration.

Figure 12. Flow visualization for baseline configuration and configurations with add-on devices.
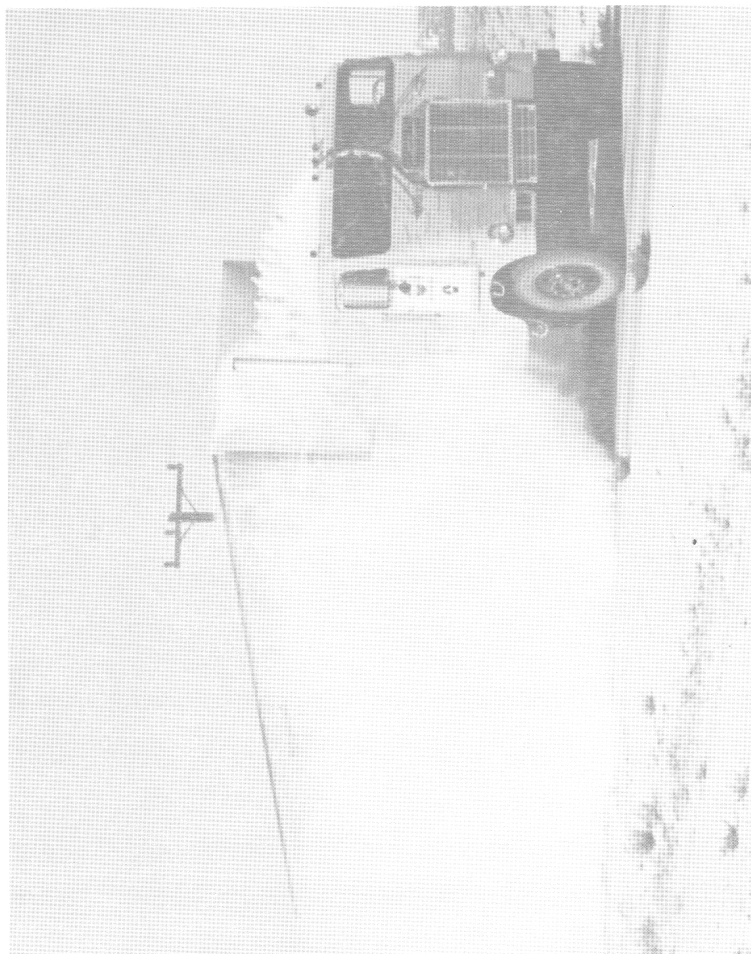
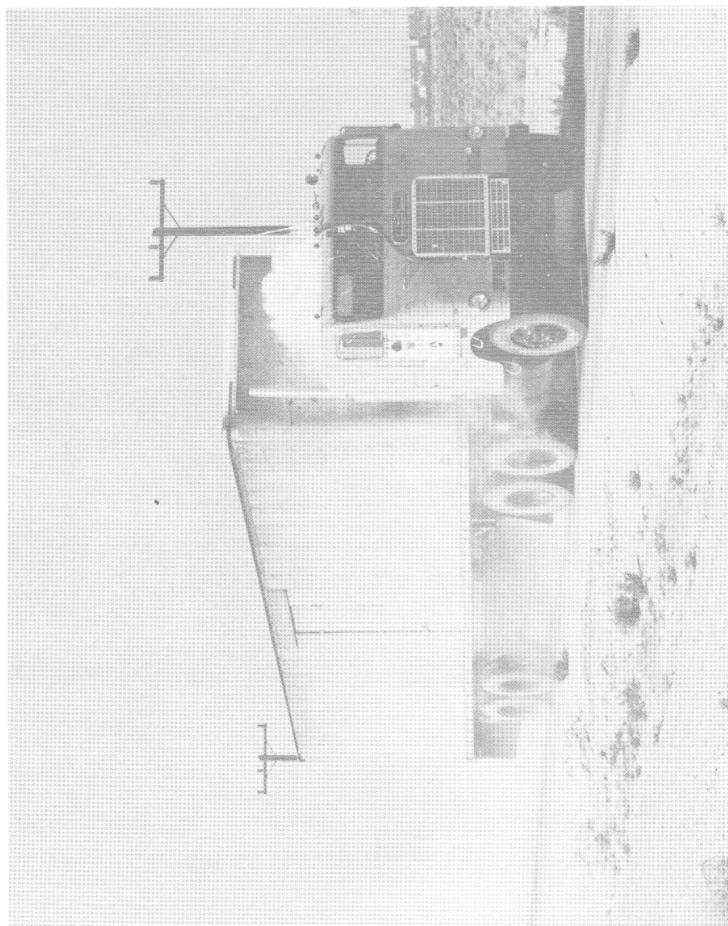(b) Device A.

Figure 12. Continued.

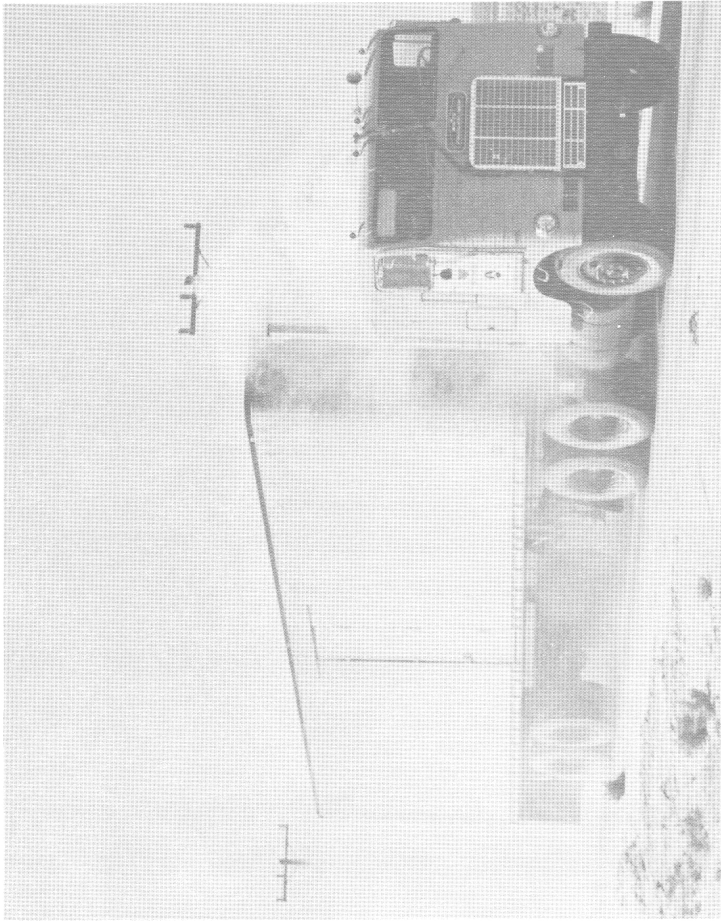(c) Device B.

Figure 12. Continued.

(d) Device C.

Figure 12. Continued.

(e) Device D.

Figure 12. Continued.

(f) Device E.

Figure 12. Concluded.